

Fire performance of brominated and halogen-free flame retardants in glass-fibre  
reinforced poly(butylene terephthalate)

M. Suzanne<sup>1</sup>, A. Ramani<sup>1</sup>, S. Ukleja<sup>1</sup>, M. McKee<sup>1</sup>, J. Zhang<sup>1,\*</sup>, M.A. Delichatsios<sup>1</sup>, P Patel<sup>2</sup>,  
P. Clarke<sup>2</sup>, P Cusack<sup>2</sup>

<sup>1</sup> FireSERT, School of Built Environment and Built Environment Research Institute,  
University of Ulster, Newtownabbey, BT37 0QB, Northern Ireland

<sup>2</sup> ITRI, Unit 3, Curo Park, Frogmore, St. Albans, Hertfordshire, AL2 2DD, UK

\* Corresponding author:

Jianping Zhang

Tel.: +44 (0)28 90366460

Email: [j.zhang@ulster.ac.uk](mailto:j.zhang@ulster.ac.uk)

Postal address: FireSERT, School of the Built Environment, Ulster University,  
Newtownabbey, BT37 0QB, UK

## **ABSTRACT**

This paper investigates the effects of brominated and halogen-free fire retardants on the fire performance of glass-fibre reinforced poly(butylene terephthalate). Brominated polystyrene was used as the brominated fire retardant (BRF) whereas aluminium diethylphosphinate (Alpi) with/without nanoclay as halogen-free fire retardants (HFFRs). Tests were conducted using thermogravimetric analysis (TGA), limiting oxygen index (LOI), UL94 and the cone calorimeter. TGA results show that decomposition of glass-fibre plus PBT (PBT+GF) starts earlier in the presence of all fire retardants (FRs). In the cone calorimeter, all FRs reduce significantly the heat release rate (HRR) compared to PBT+GF, with brominated polystyrene achieving lowest HRR primarily because bromine released in the pyrolysis gases inhibits combustion. Brominated polystyrene does not however affect the mass loss rate (MLR). Alpi alone has significant effects on reduction of both HRR and MLR which become considerably more when combined with nanoclay. It was also found that the combustion efficiency of the brominated polystyrene compound is much lower than that of HFFRs, indicating that brominated polystyrene has higher gas phase flame retardant efficiency compared to HFFRs because of the bromine radicals released during degradation of brominated polystyrene effectively quench the chemical reactions of the pyrolysis gases due to degradation of PBT.

**Keywords:** brominated fire retardants, halogen-free fire retardants, LOI, UL94, thermogravimetric analysis, cone calorimeter

## **1. INTRODUCTION**

Brominated fire retardants (BFRs) are widely used in the plastics industry to improve the fire resistance of the plastics in that they hardly impair the plastics characteristics, are very effective in relatively low amounts compared to other types of FRs, and are relatively cheap.

Unfortunately, some of the BFRs have unintended effects on the environment and human health. The environmental and toxicological hazards of a specific type of BFRs, Polybrominated diphenyl ethers (PBDEs), have been subject to extensive studies [1-6]. It was demonstrated in [1-4] that some of the PBDEs result in a strong bioaccumulation in aquatic and terrestrial food chains, and that a growing number of PBDEs is found in increasing concentrations in the human food chain, human tissues and breast milk. Furthermore, PBDEs have also been found in indoor environment such as in dust at homes [5]. Brain and nervous system were identified as one of the most vulnerable targets for the toxic actions of PBDEs [6]. The endocrine disruptive properties and particularly the neurotoxic potential of PBDEs, in combination with their environmental persistence and the risk of accumulation in tissues and (neuronal) cells have led to a ban on the production and use of PBDEs.

Whilst the main concern for BFRs comes from PBDEs, European risk assessments for other BFRs such as hexabromocyclododecane (HBCD) and tetrabromobisphenol A (TBBPA) are currently being carried out. It may be expected that HBCD will follow the same route to a ban as the PBDEs as it is a strongly bioaccumulating compound. TBBPA has better chances for ongoing production, as its bioaccumulation is less severe, but its endocrine effects (e.g. on the thyroid function) may be stronger, so lower concentrations may show already effects.

Based on existing knowledge and ongoing research, it is not surprising that some of BFRs are or will be soon phased out. Consequently, it is essential, for ecological and economical reasons, to investigate available environmental friendly alternatives. However, banning specific BFRs may imply a serious risk if the introduction of non-brominated alternatives is not properly assessed regarding environment and human health. It is also of vital importance

that substitution options do not affect the functionality and reliability of the end products, with fire behaviour being one of these aspects.

This paper presents an evaluation of alternatives for brominated polystyrene in glass-fibre reinforced poly(butylene terephthalate) (PBT+GF) for its fire retardancy. PBT+GF was fire retarded with either brominated polystyrene combined with antimony trioxide or aluminium diethylphosphinate (Alpi) with/without organically modified montmorillonite clay (OMMT). It is worthwhile to note that the brominated polystyrene used in this work represents a specific type of BFRs. Its high molecular weight means that it cannot penetrate human cell membranes or spread in the environment. Its impact on toxicity and the entrainment is still subject to further study. In this work, thermal decomposition and flammability tests of these materials were conducted using thermogravimetric analysis (TGA), limiting oxygen index (LOI), UL94 and the cone calorimeter in both horizontal and vertical orientations.

Flammability properties are determined together with comparative analyses made for all formulations in terms of mass loss in TGA and time to ignition, heat release rate, mass loss rate, production of carbon monoxide and smoke in the cone calorimeter.

The paper is organised in the following way. Firstly, the materials' information is given, along with experimental details. Next, experimental results and discussions are presented followed by the conclusions of this work.

## **2. MATERIALS**

In total, four formulations were investigated as shown in Table 1. The base formulation, PG1, consists of PBT reinforced with 30 wt. % of glass-fibre. A halogenated formulation, PG2, contains 10 wt. % brominated polystyrene (BrPS), with 5 wt. % antimony trioxide for

synergism as normally done. In addition, two halogen-free flame retardants (HFFRs) were studied: PG4 contains 15 wt. % aluminium diethylphosphinate (Alpi) and PG3 contains 15.5 wt. % Alpi with 2.5 wt. % organically modified montmorillonite clay (OMMT).

Prior to extrusion, the virgin polymer and fire retardants were dried at 120°C under vacuum in an oven for 6 hours. A Prism Twin Screw Extruder (TSE) 16 TC was used to produce the samples in the cone calorimeter. The temperatures corresponding to the rear, centre and front zones were 240 °C, 245 °C and 255 °C, respectively and the screw speed was set at 60 rpm. The extruded polymer was then pelletised and dried. A BOY 22M injection moulding machine was utilised to mould the samples. The temperatures corresponding to the rear, centre, front and nozzle zones were 240°C, 250°C, 250°C, and 260°C, respectively. These temperatures were varied by  $\pm 5^\circ\text{C}$  depending on the level for the fire retardant. The melt temperature was 255°C and the water-cooled mould was set at 80°C. The thickness of the cone samples is 2.9 mm with a surface area of 0.1 x 0.1 m<sup>2</sup>. No measurements of the polydispersity of nanoparticles were made.

## **4. EXPERIMENTAL DETAILS**

### **4.1 TGA**

Thermal analysis was performed using a Mettler Toledo TGA/STDA 851e measuring module, with temperature accuracy and temperature reproducibility of  $\pm 0.5^\circ\text{C}$ . Samples of around 10 mg were heated in alumina pans at three heating rates, i.e., 5, 10 and 20 °C/min, from 300 to 1000 °C in nitrogen with a flow rate of 50 cm<sup>3</sup>/min.

### **4.2 Limiting oxygen index (LOI) and UL94**

LOI measurements and UL94 vertical tests were conducted using 3.2 mm thick samples, according to BS EN 60695-11-10 and BS EN ISO 4589-2, respectively.

### **4.3 Cone calorimeter**

Tests were conducted at six heat fluxes in horizontal orientation (22.5, 30, 45, 60, 75 and 90 kW/m<sup>2</sup>) and one in vertical orientation (75 kW/m<sup>2</sup>). The vertical tests were conducted in order to assess the strength of the char and the effects of orientation. The exposed surface of the plates was covered with carbon black to ensure maximum surface absorption of external heat with absorptivity close to one. Before the tests, all samples were kept in a conditioning room maintained at an atmosphere of  $50 \pm 5\%$  of relative humidity and at  $23 \pm 2^\circ\text{C}$  until their mass was stabilized. All the experiments were carried out with an insulation consisting of four layers of low-conductivity Cotronic paper at the back and sides of the specimen in order to reduce heat losses to the sample holder [7]. Aluminium foil was used to avoid melted polymer to soak into the Cotronic insulation paper. At each heat flux, tests were repeated three times to ensure repeatability. Time to ignition (TTI), heat release rate (HRR), mass loss rate (MLR) and production of carbon monoxide, carbon dioxide and smoke were recorded.

## **5. RESULTS AND DISCUSSIONS**

### **5.1 TGA**

Figure 1 shows a comparison of the mass loss (TGA) curves between pure PBT and that modified with glass-fibre (PG1) at 10 °C/min. Note that for comparison purpose the weight loss of PG1 was normalised by the initial weight of PBT in PG1. It can be clearly seen that both materials undergo one-step reaction at the same temperature range. The fact that glass-fibre does not change the decomposition behaviour of PBT confirms that it is a chemically

inert material which only acts, as seen in the cone calorimeter experiments, as a protection layer in the solid phase.

Figure 2 presents a comparison of the mass loss (TGA) and mass loss rate (DTG) curves at 10 °C/min for the four formulations. The results at other heating rates are similar indicating the same pyrolysis kinetics. It seems that all FRs induce early decomposition of PBT, which may indicate that there is interaction between the FRs and PBT+GF as both neat brominated polystyrene and Alpi degrade at higher temperatures as shown in Fig. 3. The present results is consistent with the finding in [8], in which the interaction between brominated polycarbonate and PBT+GF was reported.

Table 2 shows the residue (wt. %) in TGA at 500 and 1000 °C. PG2 gives a residue of 33.0 and 29.1 wt % at 500 and 1000°C, respectively (see Table 2). This formulation contains less glass-fibre than PG1, i.e. 25.5% (85% of PBT+GF × 30 % of GF) which composes the major part of the residue. As shown in Fig. 3, BrPS degrades almost completely, and only a small amount of antimony trioxide acts in the solid phase (via SbOBr which facilitates the dissociation of C-Br bonds [9]). Consequently, as the amount of residue of PG2 is higher than expected, it is concluded that there is an interaction between PBT and BrPS which increases the amount of residue at 500 and 1000°C as shown in Table 2.

For Alpi containing materials, an additional decomposition step is observed at around 475 °C, which is due to the vaporisation of Alpi as shown in Fig. 3. It was reported in [9] that the decomposition process of Alpi depends on experimental conditions (such as the size of the crucible and the mass of the sample) and that two different decomposition behaviours are observed depending on these conditions: vaporisation of Alpi as a complete molecule (around

750K) or decomposition of Alpi (710K). The amount of residue changes depending on the process. In our measurement for PG4, the second step at 475°C is due to the vaporisation of Alpi while the change in weight slope during the first decomposition and the increase in residue are due to the action of decomposition products of Alpi.

The results of PG3 are similar to those of PG4, indicating that nanoclay does not affect the decomposition of the materials. As shown in [10-12], the primary effect of nanoclay is that it forms a protection char layer for neat polymers or enhances the char strength of FRs or intumescent coating and such physical actions of nanoclay cannot be observed for the thermally thin materials as tested by TGA; consequently, the effect of nanoclay is minimal in microscale experiments. However, as it will be shown in the cone calorimeter results, nanoclay can have a significant effect on the fire retardancy when combined with Alpi.

## **5.2 Limiting oxygen index (LOI) and UL94**

Table 3 summaries the LOI and UL94 results. The three fire retardants containing formulations are V0 rated while PG1 failed the UL94 test. This result highlights one of the drawbacks of the UL94 test as it cannot differentiate the behaviour of different fire retardants having the same acceptable V0 rating. For the LOI measurements, PG4 has the highest LOI (35.5%), followed by PG3 (31.5%), PG2 (28%) and PG1 (19.5%). The fact that Alpi alone achieves a higher LOI than Alpi combined with OMMT is somehow unexpected. This result indicates that although LOI measurement provides a numerical result convenient to rank materials, it does not correspond to an intrinsic material property and the LOI value depends on experimental characteristics such as effective heat of pyrolysis and effective heat transfer coefficient to the sample for instance [13].

### 5.3 Cone calorimeter

#### 5.3.1 Visual observations

After the tests, sample residues present different visual aspects depending on both the formulation and the external heat flux to which the samples were exposed to. For PG1 and PG2, small pores are visible on the surface of the residue and colour goes from white (high heat fluxes) to dark grey (below  $30\text{kW/m}^2$ ). These residues are mainly composed of glass-fibre, as the weight of the residue is the same as the initial glass-fibre content. For PG3 and PG4, black residues were observed: for PG4, this carbonaceous char is bumpy and porous whereas it is smooth and stiff for PG3. Observed carbonaceous chars for PG3 and PG4 are an indication of solid phase action of Alpi and OMMT.

#### 5.3.2 Time to ignition

Table 4 summarises the average times to ignition (TTIs) in horizontal configuration. At heat fluxes lower than  $45\text{kW/m}^2$ , flashes were often observed prior to sustained combustion. The ignition behaviour of PG2 is noticeably different at these low heat fluxes—flashes were still observed but the sparkle igniter had to be maintained much longer after first flames appeared in order to reach sustained combustion. This illustrates the gas phase action of BrPS contained in PG2. At lower heat fluxes, all FRs seem efficient in delaying ignition. For PG2 and PG3, an increase of about 30% in TTI is observed at  $22.5\text{kW/m}^2$  and 40% for PG4, compared to PG1. However, at higher heat fluxes PG2 actually has lower TTIs than PG1, indicating that the action of BrPS on TTI is less efficient than that observed for Alpi or Alpi combined with OMMT. Similar findings were reported in [14,15], which showed that Alpi increases TTI of PBT+GF.

### 5.3.3 Mass loss rate

Figure 4 shows a comparison of the mass loss rate histories at  $60 \text{ kW/m}^2$  between the four formulations. The trends of the MLR follow those of typical charring materials. Namely, the mass loss rate 1) increases to reach the first peak, 2) decreases rapidly to reach a plateau, 3) increases again to form the second peak and 4) finally decreases when most of the fuel is consumed. The decrease of the mass loss rate after the first peak is due to the formation of a surface shield as a result of accumulation of glass-fibre on the surface [16]. It reduces the pyrolysis gas supply to the combustion zone by retarding heat transfer from the surface material to the virgin zone owing to re-radiation losses from the surface consisting mainly of glass-fibre. The second peak is due to the insulated backside. When heat reaches the insulated back surface, there is an accumulation of energy due to the insulation, which results in an increase of the mass loss rate.

The MLRs of PG1 and PG2 are similar, which indicates that the BrPS combined with  $\text{Sb}_2\text{O}_3$  has negligible effect in the solid phase. For PG4, a thin char layer is formed on the sample surface, which could be responsible for the reduction in the first peak MLR. When OMMT is added, the MLR is reduced further by between 30 and 50% depending on the external heat flux owing to the increased strength of the char formed by glass-fibre and Alpi in the presence of OMMT. The pyrolysis process is however prolonged because the total mass loss is similar between PG3 and PG4. A much rigid and solid-like char was observed for PG3 compared to the thin char layer for PG4.

### 5.3.4 Heat release rate

Figure 5 shows the HRR (normalised by the exposed surface area) histories at  $60 \text{ kW/m}^2$ . The results at other heat fluxes have similar trends and thus are not shown here for brevity.

Interestingly, while the mass loss rates of PG1 and PG2 are similar (see Fig. 4), their heat release rates are considerably different. BrPS reduces the first peak HRR by more than 70%. This result indicates a strong gas phase action of BrPS, which consists in interacting of bromine with highly reactive free-radical species such as H• and O• by slowing down or stopping the cascade-chain mechanism of the combustion [17]. Antimony trioxide interacts with BrPS and improve the decomposition of the FR. PG2 produces the lowest HRRs among all formulations at all heat fluxes considered without prolonging the burning process compared to PG1.

For PG4, there is a reduction of about 60% at its first peak. However, the second peak HRR is similar between PG1 and PG4. The present results are similar to those reported in [9], where a decrease of about 45% in the first peak HRR was achieved whilst no difference was noted for the second peak HRR when 20% Alpi was used in PBT+GF.

For PG3, there is a further reduction of the HRR compared to PG4. The first peak HRR for PG3 is comparable with that for PG2, however with a prolonged burning process. The reduction of the HRRs by PG3 in comparison to PG4 is mainly due to the reduction in the MLR as shown in Fig. 4.

### ***5.3.5 Effective heat of combustion $\Delta H_{c,eff}$***

Figure 6 presents the effective heat of combustion (EHoC), calculated by dividing the total heat released (THR) by the total mass lost and then normalised by the PBT+GF weight content for each formulation. PG1 has the highest EHoC with an average of 15.5 kJ/g. PG2 has the lowest EHoC ranging from 5.6 to 8.8 kJ/g depending on the external heat flux. It corresponds to a decrease of about 55% compared to PG1. This decrease illustrates the

dominant gas phase action of BrPS. Although the total mass loss for PG2 is the same for all heat fluxes, EHoC increases slightly with the external heat flux. The efficiency of the gas phase action of BrPS seems to decrease with increasing heat flux. The gas phase action of BrPS is also illustrated by the difficulty in igniting PG2 samples described previously and local extinction at lowest heat fluxes. PG4 shows a decrease of about 15% in EHoC which also indicates an action of the phosphorous FR in the gaseous phase with similar results reported in [9]. PG3 has a similar EHoC to PG4 although PG3 burning process lasts longer with lower MLR. OMMT reduces the HRR but does not change the total amount of heat released. The action of the OMMT is only physical. It should be mentioned that the values obtained in this work are slightly lower than those reported in the literature. For example, 22 kJ/g was reported in [17] for pure PBT and 21 kJ/g for PBT+GF [14]. This difference could be due to the difference in the samples used in these studies as glass-fibre should not have any influences other than physical on the fire behaviour.

### ***5.3.6 Production of smoke and carbon monoxide***

Carbon monoxide, and smoke yields were calculated from the pre-ignition period until the flame goes out. The smoke production rate was calculated as the volume flow rate in the exhaust duct times the extinction coefficient. Results are plotted in Figs. 7-9.

As expected, PG1 has the lowest CO and smoke yields and production rates. It demonstrates a more complete combustion than the other three formulations. The combustion of PG2 yields about 20% more smoke than other FR formulations and 55% more than PG1. Its peak values of smoke production rates are 2.5 times higher than those obtained for PG1. PG4 yields more than 15% of CO than PG2 and almost 80% more than PG1. CO is produced 15% more by PG4 than by PG2. It is generally considered that an increase in smoke and CO production by

a factor of more than two is the consequence of a suppressed total oxidation process and is synonym of a radical trapping mechanism. Consequently, BrPS and Alpi may act in the gas phase as radical scavengers. When OMMT is combined with Alpi in PG3, the same amount of CO and smoke is produced as when Alpi is used alone. However, the use of OMMT reduces the rate at which these species are released by 45% and 25% for CO and smoke respectively.

### ***5.3.7. Modelling of pyrolysis of PBT+GF***

By plotting the time to ignition against the heat flux it is possible to determine the effective ignition and flammability properties [19]. The results are summarised in Table 5. As mentioned earlier, the action of glass-fibre can be considered similar to that of a char layer, which allows the prediction of the pyrolysis rate of PBT+GF using the methodology that the authors have previously developed for polymer nanocomposites [10]. A brief description of the methodology is given below whereas detailed formulations can be found in [10].

Due to the shielding effect of glass-fibre, the heat flux on the interface of the glass-fibre surface layer and virgin material only a fraction of the heat flux on the surface for the case when there is no surface layer. This allow to define a heat flux ratio [10], i.e. the ratio of the heat flux on the surface for the case when there is no surface layer to that at the interface for the case of PBT+GF. By definition, this heat flux ratio should be equal to or larger than one. This heat flux ratio can be calculated by solving 1D conduction equation with the use of the experiment mass loss data and effective ignition and flammability properties given in Table 5. In the calculations, the heat of pyrolysis of PG1+GF was assumed to be the same as that of

pure PBT [20], i.e., 1000 kJ/kg, because glass-fibre does not affect decomposition of PBT as confirmed in the TGA results.

The calculated heat flux ratio is plotted against the pyrolysed depth (i.e., the depth of the material that has pyrolysed) in Fig. 10 for a heat flux of 60kW/m<sup>2</sup>, where we note that it is nearly one at the beginning because the surface layer is very thin and then increases almost linearly after the initial stage. This result implies that the reduction of the heat flux at the interface is proportional to the amount of glass-fibre on the surface. Using curving fitting, the following relationship between the heat flux ratio and pyrolysed depth was deduced.

$$\begin{aligned} \text{Ratio}_{flux} &= 1 && \text{for } \delta_{pyro} < 0.8\text{mm} \\ \text{Ratio}_{flux} &= 1.25\delta_{pyro} && \text{for } \delta_{pyro} > 0.8\text{mm} \end{aligned} \quad (1)$$

Subsequently, Equation 1, along with the effective properties, can be used to predict the pyrolysis rate at other heat fluxes [10]. In Fig. 11, the predicted pyrolysis rates are compared to the experimental ones. The trends of the two sets of data are similar and the predictions are also in reasonably quantitative agreement with the measurements. This result confirms the earlier proposition that the effect of glass-fibre is similar to a char layer and its fire protection performance improves when the depth of the glass-fibre layer increases during pyrolysis.

### 5.3.8. Vertical tests

Figure 12 shows a comparison of the MLRs and HRRs at 75 kW/m<sup>2</sup> in horizontal and vertical orientations. The results show that both MLR and HRRs are about 30% lower in vertical orientation than in horizontal orientation. The action of BrPS and Alpi is however similar for both cases. The difference in two orientations could be attributed to the differences in convective heat transfer coefficient and flame radiation to the sample. For example, for tests in vertical position the flame is closer to the surface and thus the view factor is different.

However, the change in the flame heat flux alone is not sufficient to explain the decrease in mass loss rate as the flame heat flux is considered small (estimated to be about  $10\text{kW/m}^2$ ) compared to the external heat flux. Another possible explanation could be a change in the burning behaviour in vertical orientation (for example in the way how the polymer flows and pyrolyses) because a difference in the total mass loss was also observed between horizontal and vertical orientations as plotted in Fig. 13, which shows the total mass loss in vertical orientation is systematically lower than that in horizontal orientation.

## 6. CONCLUSIONS

Glass-fibre reinforced PBT was fire retarded with a brominated fire retardant (BFR), namely brominated polystyrene (BrPS) combined with antimony trioxide, and two halogen-free fire retardants (HFFRs), Alpi with and without OMMT. The fire retardancy of these compound materials was assessed using TGA, LOI, UL94 and the cone calorimeter. The major conclusions of this work are:

- All fire retardants accelerate the decomposition of pure PBT+GF in TGA indicating interaction between fire retardants and PBT+GF.
- All fire retarded formulations achieved V0 rating in the UL94 vertical test for 3.2mm thick samples, whereas the neat PBT+GF (PG1) failed the test. For LOI test, Alpi alone (PG4) has the highest LOI, followed by Alpi with OMMT (PG3), brominated polystyrene (PG2) and PG1.
- Brominated polystyrene shows action in the gas phase because the combustion is incomplete and the heat of combustion decreases. Therefore, it achieves the lowest heat release rate (HRR) among all formations with a reduction of more than 70% compare to PG1 even though it has nearly the same mass loss rate (MLR) as PG1. However, it produces excessive CO and smoke. The bromine radicals released during

degradation of brominated polystyrene effectively quenches the chemical reactions of the pyrolysis gases (and thus reduce the heat release rate) resulting in some of the pyrolysis gases not completely burned and escaped as unburned gases;

- For PG4, there is a reduction of HRR and MLR indicating that Alpi acts both in the condensed phase by modifying the residue (glass-fibre plus residue from Alpi, Figs. 4 and 5) and in the gaseous phase by decreasing the effective heat of combustion. The decrease of the HRR is however less than that by brominated polystyrene. Although the Alpi formulation produces less smoke than the brominated one (PG2), it releases more CO;
- When OMMT is combined with Alpi (PG3), there is a further reduction in the HRR and MLR. The HRR of PG3 is similar to that of PG2, as a result of reduced MLR. Yields of CO and smoke are comparable to those of PG4. The combination of Alpi and OMMT appears to be the best alternative to the brominated FR in PBT+GF because the strength and effectiveness of the residue by glass-fibre and Alpi residue increases in the presence of OMMT.
- For vertical cone calorimeter tests, lower HRRs/MLRs were recorded for all formulations possibly due to reduced flame heat flux and also a change in the burning behaviour because lower total mass loss was observed in vertical orientation. No dripping was observed for all formulations.
- The methodology previously developed for charring materials and polymer nanocomposites was used to quantify the effect of glass-fibre and to predict the pyrolysis of PG1 and the results indicated that glass-fibre acts only in the solid phase as a protection layer. The predicted pyrolysis rates are in good agreement with the measurements.

- The present study also highlights the limitations of commonly used UL94 and LOI tests, because these tests (UL94 and LOI) do not provide a way to discriminate the behaviour of these materials in real fires. For example, UL94 test cannot differentiate materials with the same rating (V0 in this case). The LOI results in this work indicate that the formulation containing only Alpi (PG4) has the highest LOI. However, the cone calorimeter results clearly show that PG2 and PG3 have similar HRRs, which are lower than those of PG4. In addition, LOI and UL94 tests cannot take into account smoke and CO production, which are important hazards in fires.

## **ACKNOWLEDGEMENTS**

The authors acknowledge the EU for financially supporting the ENFIRO project under Grant No 226563. The authors also thank Mr. W Veighey for helping with the experiments.

## **REFERENCES**

1. Hites, RA., "Polybrominated diphenyl ethers in the environment and in people: a meta-analysis of concentrations", *Environ. Sci. Technol.* 38: 945-956 (2004)
2. Fångström, B., Strid, A., Grandjean, P., Weihe, P., Bergman A., "A retrospective study of PBDEs and PCBs in human milk from the Faroe Islands", *Environ. Health* 4: 12 (2005)
3. Schecter, A., Päpke, O., Tung, K., Joseph, J., Harris, T., Dahlgren, J., "Polybrominated diphenyl ether flame retardants in the U.S. population: current levels, temporal trends, and comparison with dioxins, dibenzofurans, and polychlorinated biphenyls", *J. Occup. Environ. Med.* 47: 199-211 (2005)

4. She, J., Holden, A., Sharp, M., Tanner, M., Williams-Derry, C., Hooper, K.,  
“Polybrominated diphenyl ethers (PBDEs) and polychlorinated biphenyls (PCBs) in  
breast milk from the Pacific Northwest”, *Chemosphere* 67: S307-317 (2007)
5. Stapleton, H., Dodder, N., Offenberg, J., Schantz, M., Wise, S., “Polybrominated  
Diphenyl Ethers in house dust and clothes dryer lint” *Environmental Sci Technol.* 38  
(2004)
6. Dingemans, M., Ramakers, G., Gardoni, F., Van Kleef, R., Bergman, A., Di Luca, M.,  
Van den Berg, M., Westerink, R., Vijverberg, H., “Neonatal exposure to brominated  
flame retardant BDE-47 reduces long-term potentiation and postsynaptic protein  
levels in mouse hippocampus”, *Environ. Health Perspect.* 115: 865-870 (2008)
7. de Ris, J., Khan, M., “A sample holder for determining material properties”, *Fire and  
Materials*, 24: 219-226 (2000)
8. H. Sato, K. Kondo, S. Tsuge, H. Ohtani, N. Sato, *Polym.Degrad.Stab.* 1998, 62, 41-  
48.
9. Lewin M. (2001) Synergism and catalysis in flame retardancy of polymers, *Polymers  
for advanced technologies* 12, pp. 215-222.
10. Zhang, J., Delichatsios, M., and S. Bourbigot, Experimental and numerical study of  
the effects of nanoparticles on pyrolysis of a polyamide 6 (PA6) nanocomposite in the  
cone calorimeter, *Combustion and Flame*, 156(11):2056-62, 2009 6
11. Zhang, J., Hereid, M., Hagen, M., Bakirtzis, D., Delichatsios, M., Fina, A.,  
Castrovinci, A., Camino, G., Samyn, F., Bourbigot, S., “Effects of nanoclay and fire  
retardants on fire retardancy of a polymer blend of EVA and LDPE”, *Fire Safety J.*  
44: 504-513 (2008)

12. Zhang J, Delichatsios, M., McKee, M. and Ukleja, S. (2011) Experimental Study of burning Behaviours of Intumescent Coating and Nanoparticles Applied on Flaxboard, *Journal of Fire Science*, 29(6), 519-531
13. Suzanne, M., Delichatsios, M., Zhang, J., “Prediction of the limiting oxygen index using simple flame extinction theory and material properties obtained from bench scale measurements”, *Proc. of 10th IAFSS*.
14. Braun, U., ScharTEL, B., “Flame retardancy mechanisms of aluminium phosphinate in combination with melamine cyanurate in glass-fibre-reinforced Poly(1,4-butylene terephthalate)”, *Macromolecular materials and engineering*, 293: 206-217 (2008)
15. Braun, U., Bahr, H., Sturm, H., ScharTEL, B., “Flame retardancy mechanisms of metal phosphinates and metal phosphinates in combination with melamine cyanurate in glass-fiber reinforced poly(1,4-butylene terephthalate): the influence of metal cation”, *Polymers for advanced technologies* 19: 680-692 (2008)
16. Casu, A., Camino, G., De Giorgi, M., Flath, D., Laudi, A, Mornone, V., “Effect of glass fibres and fire retardant on the combustion behaviour of composites, glass fibres-poly(butylene terephthalate)”, *Fire and Materials* 22: 7-14 (1998)
17. Lewin, M., Weil, E., *Fire Retardant Materials*, Woodhead Publishing Ltd, 2001.
18. Brehme, S., ScharTEL, B., Goebbels, J., Fischer, O., Pospiech, D., Bykov, Y., Döring, “Phosphorus polyester versus aluminium phosphinate in poly(butylene terephthalate) (PBT): Flame retardancy performance and mechanisms”, *Polymer Degradation and Stability* 96: 875-884 (2011)
19. Delichatsios, M.A., “Piloted ignition times, critical heat fluxes and mass loss rates at reduced oxygen atmospheres”, *Fire Safety Journal* 40:197-212 (2005)

20. Zhang, J., Delicahtsios, M.A., “Further Validation of a Numerical Model for Prediction of Pyrolysis of Polymer Nanocomposites in the Cone Calorimeter”, *Fire Technology* 46:307-319 (2010)

## Tables

Table 1. Summary of the formulations and their compositions studied in this work.

Compounds	% weight of formulations				Commercial product name and suppliers
	PG1	PG2	PG3	PG4	
PBT+GF	100	85	82	85	Arnite TV4 261 from DSM
Brominated polystyrene	0	10	0	0	Milebrome 7010 from MPI Chemie
Antimony trioxide	0	5	0	0	Timonox Red Star from Chemtura
Alpi	0	0	15.5	15	Exolit OP 1230 from Clariant
OMMT	0	0	2.5	0	Cloisite 30B from Southern Clay Products

Table 2. Residue (wt %) in TGA at 500 and 1000°C

	PG1	PG2	PG3	PG4
500 °C	34.2	33	36.9	35.6
1000 °C	30.8	29.1	33.5	31.9

Table3. Results of limiting oxygen index (LOI) and UL 94 tests.

	PG1	PG2	PG3	PG4
LOI (%)	19.5	28.0	31.5	35.5
UL-94 Vertical (nom 3.2mm)	Fail	V0 Pass	V0 Pass	V0 Pass

Table 4. Averaged time to ignition at different heat fluxes in the horizontal cone calorimeter.

Formulations	22.5kW/m <sup>2</sup>	30kW/m <sup>2</sup>	45kW/m <sup>2</sup>	60kW/m <sup>2</sup>	75kW/m <sup>2</sup>	90kW/m <sup>2</sup>
PG1	228	101	44.5	26	15	12.5
PG2	335	116	43	26	12	9.7
PG3	329	158	55	32	14.5	11.2
PG4	390	150	51.5	29	16	9.3

Table 5. Effective ignition properties determined from the ignition tests in the cone calorimeter.

Formulation	$\rho$ (kg/m <sup>3</sup> )	$\alpha$ (m <sup>2</sup> /s)	$\dot{q}_{cri}''$ (kW/m <sup>2</sup> )	$T_{ig}$ (K)	$k$ (W/m.K)	$c$ (J/kg.K)	$k\rho c$ (kJ <sup>2</sup> /m <sup>4</sup> .K <sup>2</sup> .s)
PG1	1520	4.9x10 <sup>-8</sup>	12.2	647	0.17	2215	0.56
PG2	1610	5.8x10 <sup>-8</sup>	18.4	725	0.14	1490	0.33
PG3	1495	5.1x10 <sup>-8</sup>	19.9	742	0.13	1770	0.36
PG4	1490	5.5x10 <sup>-8</sup>	22.5	767	0.12	1520	0.28

## List of figures

Figure 1. Comparison of the mass loss (TGA) curves between pure PBT and glass-fibre enforced PBT (PG1) at 10 °C/min in nitrogen. The weight of PG1 was normalised by the initial weight of PBT in PG1.

Figure 2. TGA and DTG curves at 10 °C/min in nitrogen.

Figure 3. TGA curves of brominated polystyrene and Alpi (PG1 as reference).

Figure 4. Mass loss rate at 60kW/m<sup>2</sup> in the horizontal cone calorimeter.

Figure 5. Heat release rate at 60kW/m<sup>2</sup> in the horizontal cone calorimeter.

Figure 6. Comparison of effective heat of combustion (kJ/g<sub>PBT</sub>), calculated by dividing the total heat released by the PBT content in each formulation, in the horizontal cone calorimeter.

Figure 7. CO production rate (g/s) at 60kW/m<sup>2</sup> in the horizontal cone calorimeter.

Figure 8. Smoke production rate (m<sup>2</sup>/s) at 60kW/m<sup>2</sup> in the horizontal cone calorimeter

Figure 9. Average CO and smoke yields at all heat fluxes in the horizontal cone calorimeter.

Figure 10. Calculated instantaneous heat flux ratio,  $ratio_{flux}$ , against the pyrolysed depth,  $\delta_{pyro}$ , at 60 kW/m<sup>2</sup> (sample thickness is 2.9 mm). Two lines represent the best fits of the calculated results.

Figure 11. Comparisons of experimental and predicted mass loss rates of PG1 at different heat fluxes.

Figure 12. Comparison of MLRs and HRRs at 75kW/m<sup>2</sup> between horizontal and vertical tests.

Figure 13. Comparison of total mass loss (g) between horizontal and vertical tests.

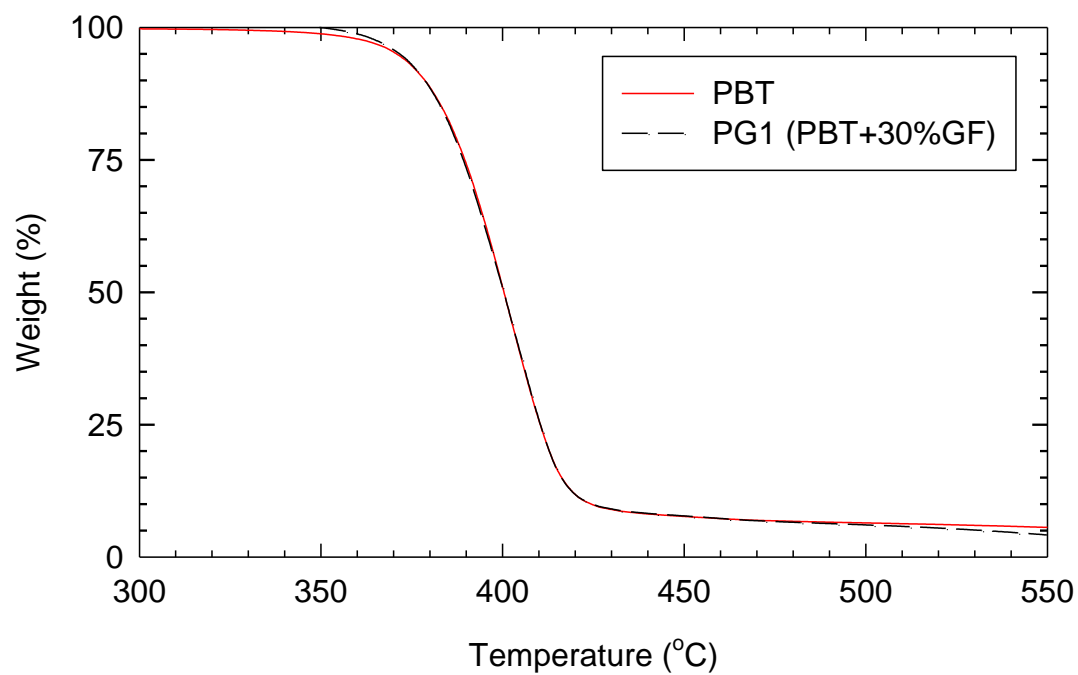
**Figures**

Figure 1. Comparison of the mass loss (TGA) curves between pure PBT and glass-fibre enforced PBT (PG1) at 10 °C/min in nitrogen. The weight of PG1 was normalised by the initial weight of PBT in PG1.

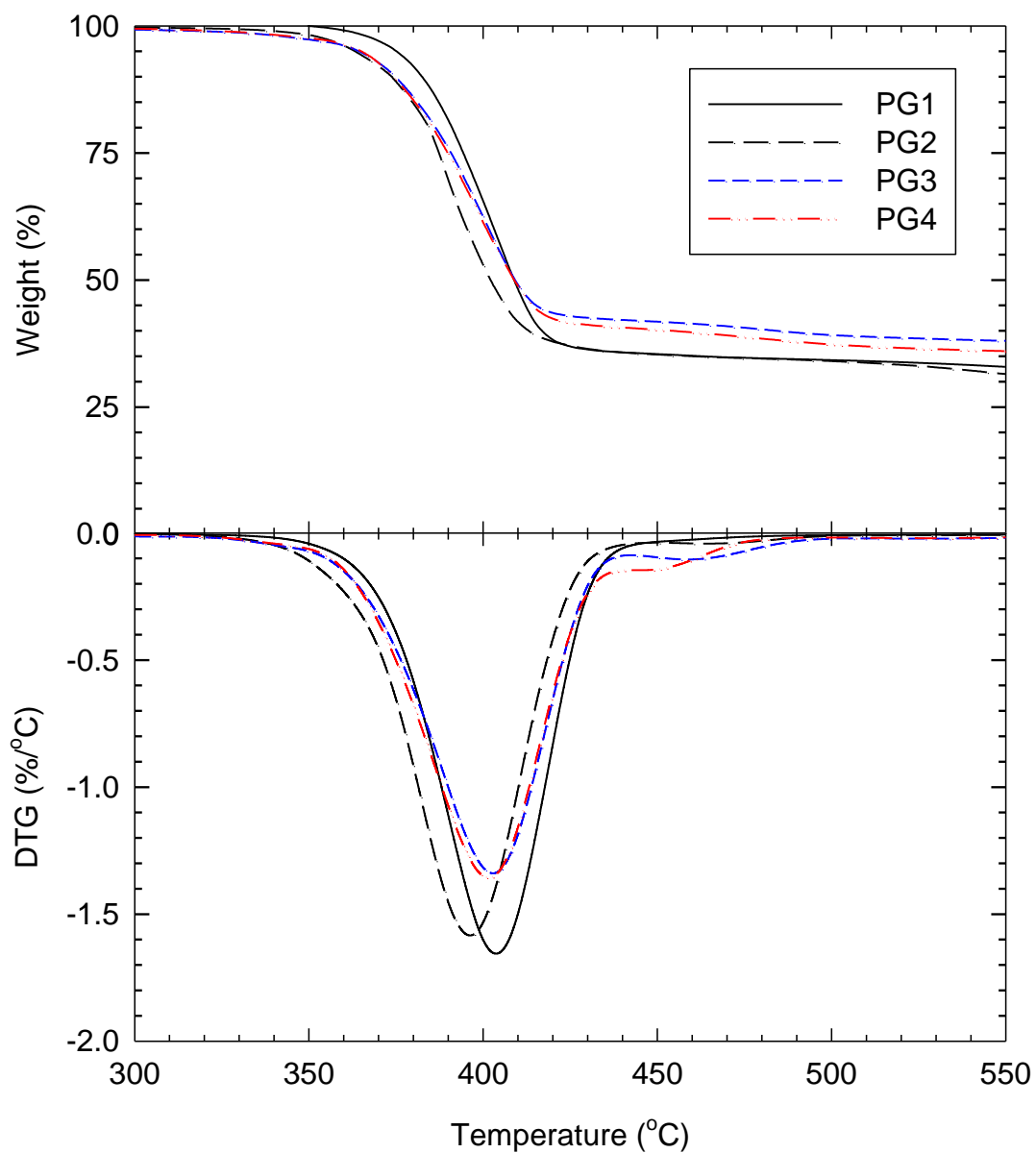


Figure 2. TGA and DTG curves at 10 °C/min in nitrogen.

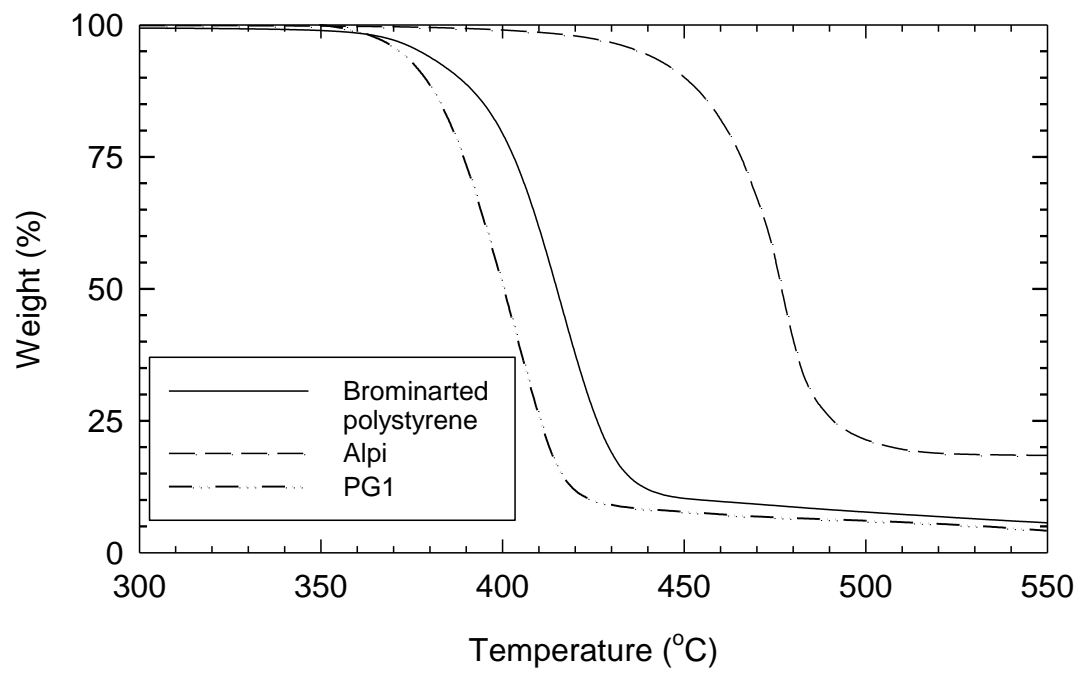


Figure 3. TGA curves of brominated polystyrene and Alpi (PG1 as reference).

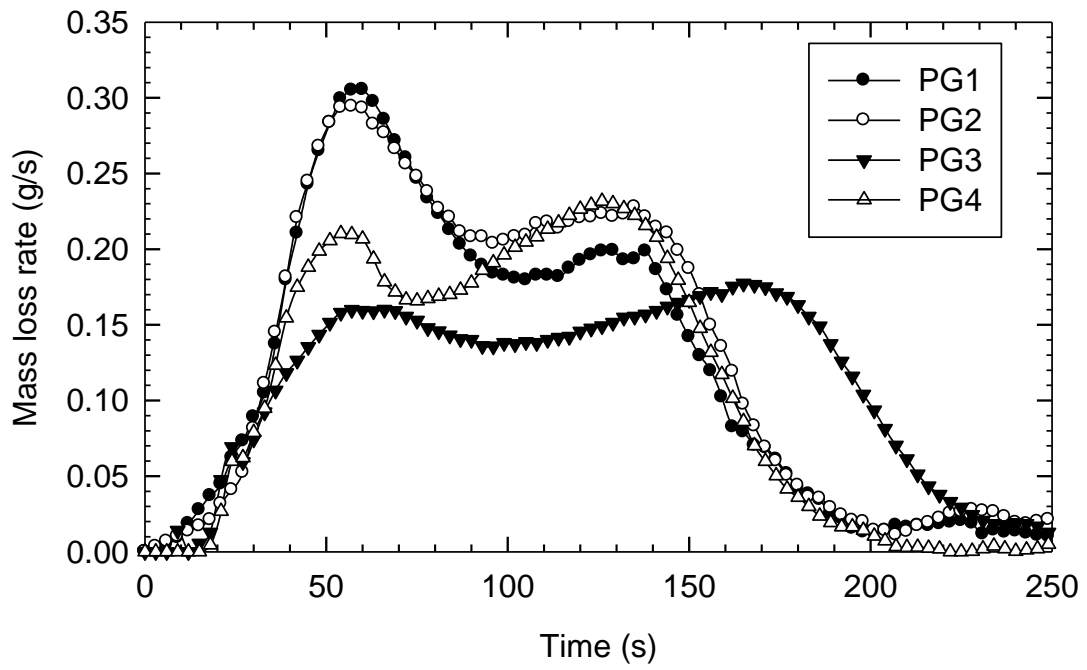


Figure 4. Mass loss rate at  $60\text{kW/m}^2$  in the horizontal cone calorimeter.

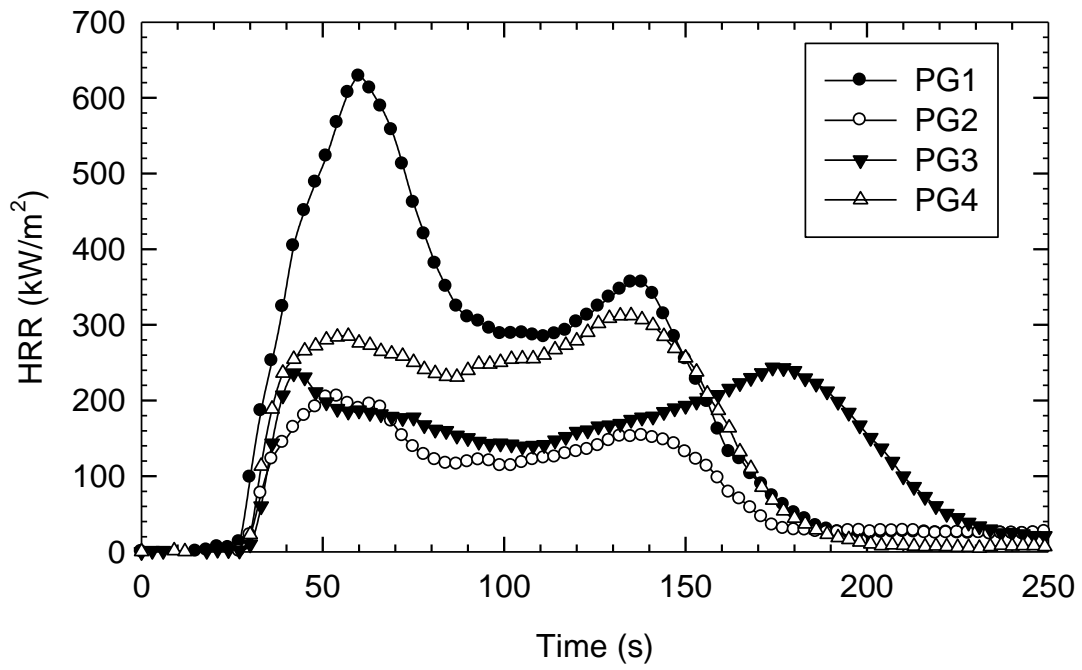


Figure 5. Heat release rate at 60kW/m<sup>2</sup> in the horizontal cone calorimeter.

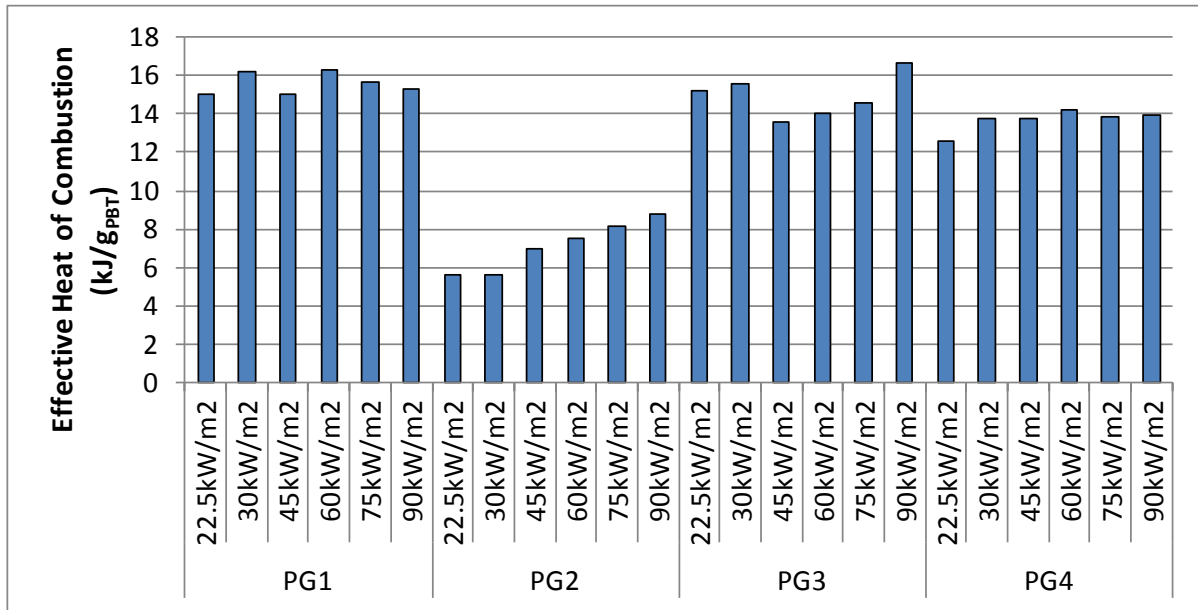


Figure 6. Comparison of effective heat of combustion (kJ/g<sub>PBT</sub>), calculated by dividing the total heat released by the PBT content in each formulation, in the horizontal cone calorimeter.

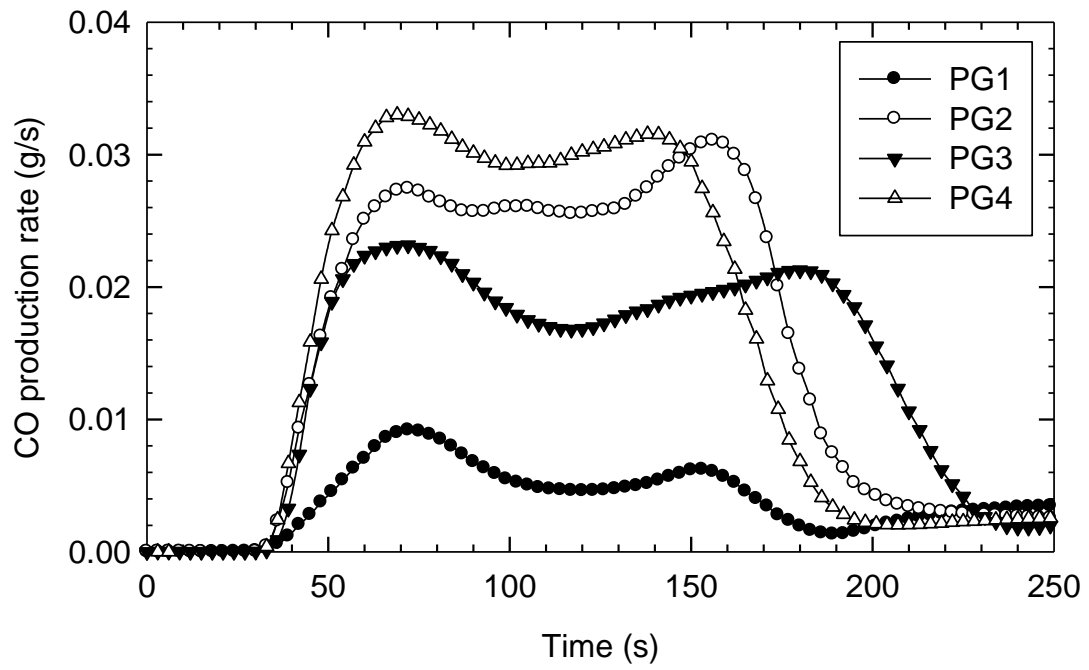


Figure 7. CO production rate (g/s) at 60kW/m<sup>2</sup> in the horizontal cone calorimeter.

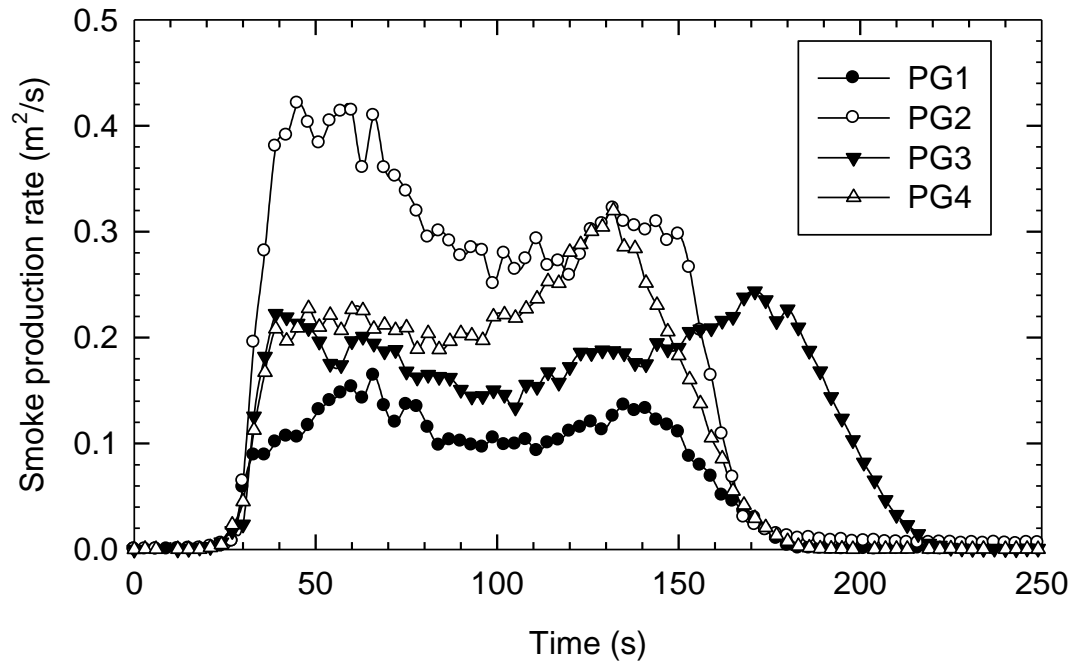


Figure 8. Smoke production rate ( $\text{m}^2/\text{s}$ ) at  $60\text{kW}/\text{m}^2$  in the horizontal cone calorimeter.

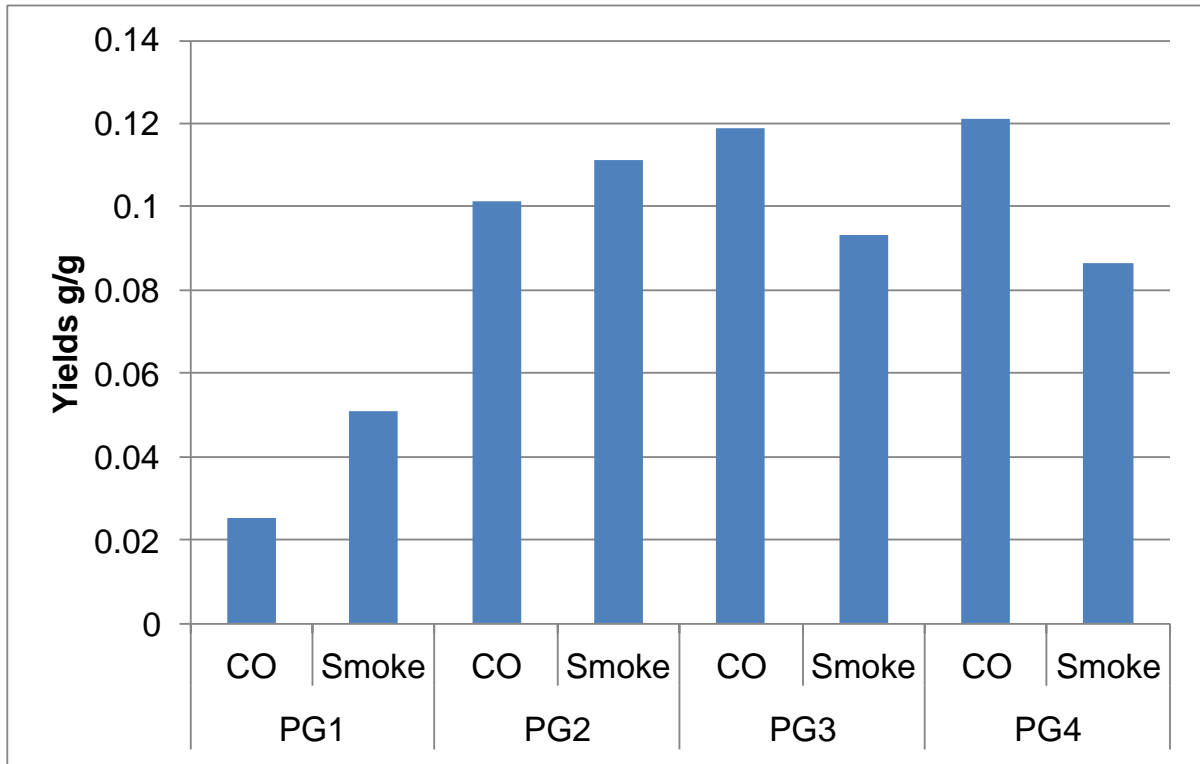


Figure 9. Average CO and smoke yields at all heat fluxes in the horizontal cone calorimeter.

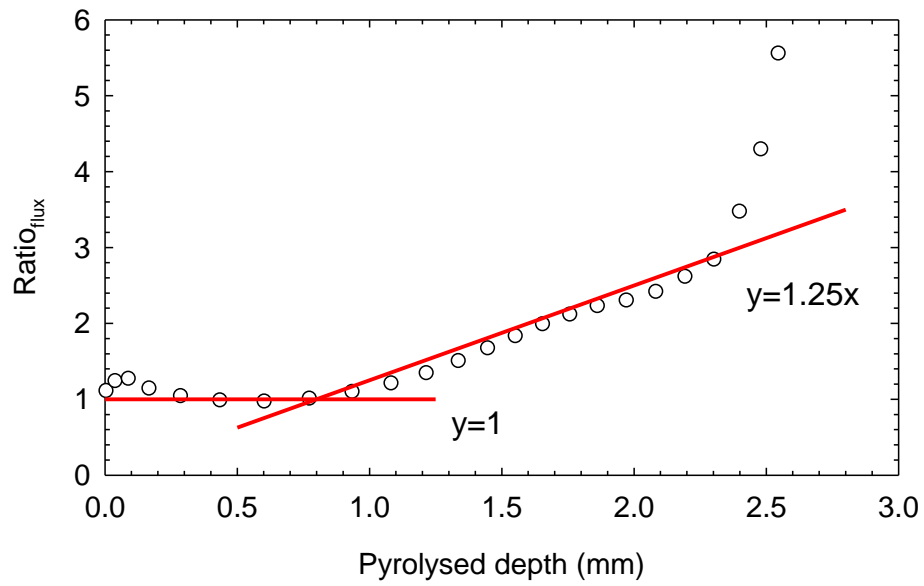


Figure 10. Calculated instantaneous heat flux ratio,  $ratio_{flux}$ , against the pyrolysed depth,  $\delta_{pyro}$ , at  $60 \text{ kW/m}^2$  (sample thickness is  $2.9 \text{ mm}$ ). Two lines represent the best fits of the calculated results.

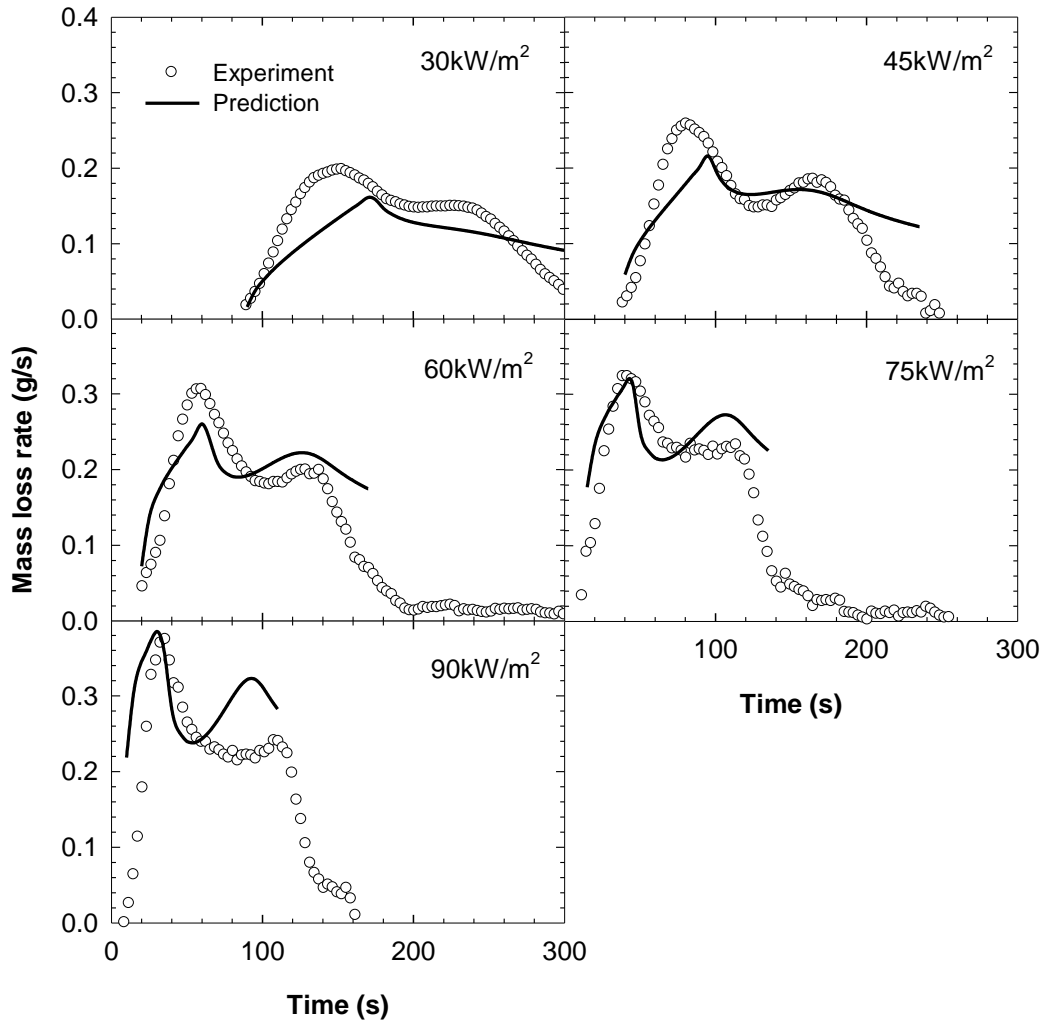


Figure 11. Comparisons of experimental and predicted mass loss rates of PG1 at different heat fluxes.

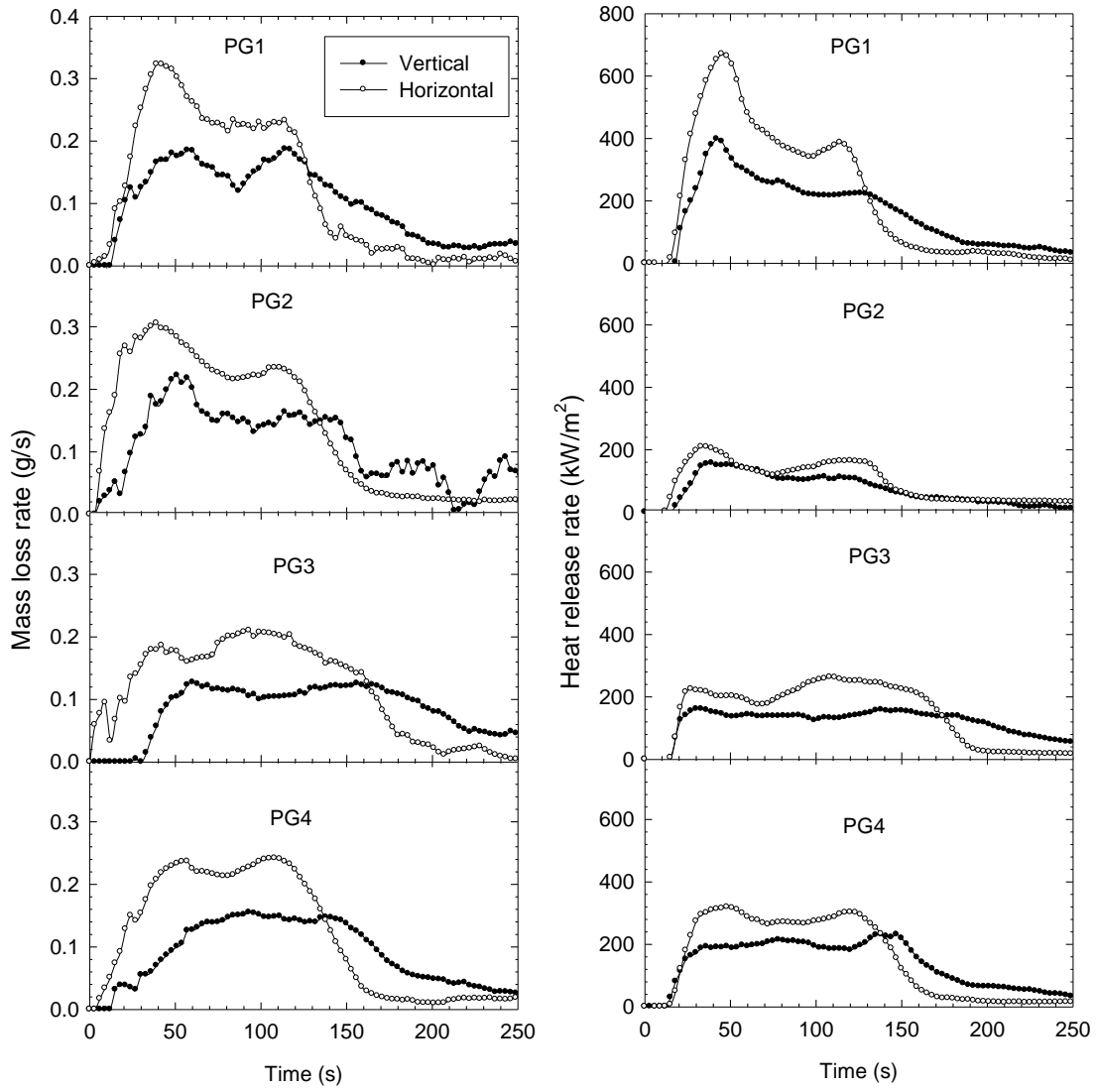


Figure 12. Comparison of MLRs and HRRs at 75kW/m<sup>2</sup> between horizontal and vertical tests.

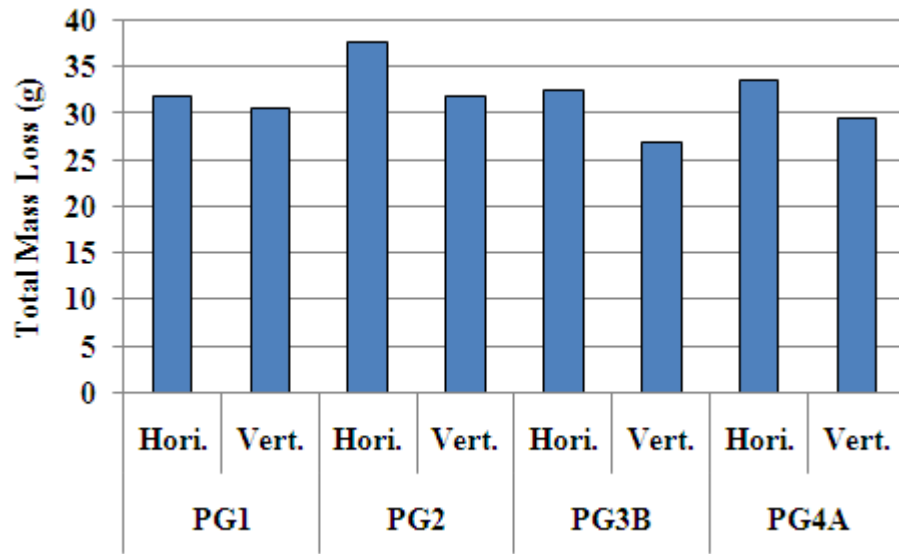


Figure 13. Comparison of total mass loss (g) between horizontal and vertical tests.